
Influence-Based Mini-Batching for Graph Neural Networks

Anonymous Author(s)

Anonymous Affiliation

Anonymous Email

Abstract

Using graph neural networks for large graphs is challenging since there is no clear way of constructing mini-batches. To solve this, previous methods have relied on sampling or graph clustering. While these approaches often lead to good training convergence, they introduce significant overhead due to expensive random data accesses and perform poorly during inference. In this work we instead focus on model behavior during inference. We theoretically model batch construction via maximizing the influence score of nodes on the outputs. This formulation leads to optimal approximation of the output when we do not have knowledge of the trained model. We call the resulting method influence-based mini-batching (IBMB). IBMB accelerates inference by up to 130x compared to previous methods that reach similar accuracy. Remarkably, with adaptive optimization and the right training schedule IBMB can also substantially accelerate training, thanks to precomputed batches and consecutive memory accesses. This results in up to 18x faster training per epoch and up to 17x faster convergence per runtime compared to previous methods.

1 Introduction

Creating mini-batches is highly non-trivial for connected data, since it requires selecting a meaningful subset despite the data's connectedness. When the graph does not fit into memory, the mini-batching problem is equally relevant for both inference and training. However, mini-batching methods have so far mostly been focused on training, despite the major practical importance of inference. Once a model is put into production, it continuously runs inference to serve user queries. On AWS, more than 90 % of infrastructure cost is due to inference, and less than 10 % is due to training [24]. Even during training, inference is necessary for early stopping and performance monitoring. A training method thus has rather limited utility by itself.

Selecting mini-batches for inference is distinctly different from training. Instead of averaging out stochastic sampling effects over many training steps, we need to ensure that every prediction is as accurate as possible. To achieve this, we propose a theoretical framework for creating mini-batches based on the expected influence of nodes on the outputs. Selecting nodes according to this formulation provably leads to an optimal approximation of the output. The resulting optimization problem shows that we need to distinguish between two classes of nodes: Output nodes and auxiliary nodes. Output nodes are those for which we compute a prediction *in this batch*, for example a set of validation nodes. Auxiliary nodes provide inputs and define the batch's subgraph. This distinction allows us to choose a meaningful neighborhood for every prediction, while ignoring irrelevant parts of the graph. Note that output nodes in one batch can be auxiliary nodes in another batch.

This distinction furthermore splits mini-batching into two problems: 1. How do we partition output nodes into efficient mini-batches? 2. How do we choose the auxiliary nodes for a given set of output nodes? Having split the problem like this, we see that most previous works either focus exclusively on the first question by only using graph partitions [7] or on the second question and choose a uniformly random subset of nodes as output nodes [21, 42]. Jointly considering both aspects with an overarching theoretical framework allows for substantial synergy effects. For example, batching nearby output nodes together allows one output node to leverage another one's auxiliary nodes.

We call this overall framework influence-based mini-batching (IBMB). On the practical side, we propose two instantiations of IBMB by approximating the influence between nodes via personalized

44 PageRank (PPR). We use fast approximations of PPR to select auxiliary nodes by their highest
 45 PPR scores. Accordingly, we partition output nodes using PPR-based node distances or via graph
 46 partitioning. We then use the subgraph induced by these nodes as a mini-batch. IBMB accelerates
 47 inference by up to 130x compared to previous methods that achieve similar accuracy.

48 Remarkably, we found that IBMB also works well for training, despite being derived from inference.
 49 This is due to the computational advantage of precomputed mini-batches, which can be loaded from
 50 a cache to ensure efficient memory accesses. We counteract the negative effect of the resulting sparse
 51 mini-batch gradients via adaptive optimization and batch scheduling. Overall, IBMB achieves an up
 52 to 18x improvement in time per training epoch, with similar final accuracy. This fast runtime more
 53 than makes up for any slow-down in convergence per step. Its speed advantage grows even further
 54 for the common setting of low label ratios, since our method avoids computation on irrelevant parts
 55 of the graph. Our implementation is available online¹. In summary, our core contributions are:

- 56 • Influence-based mini-batching (IBMB): A theoretical framework for selecting mini-batches for
 57 GNN inference based on influence scores.
- 58 • Practical instantiations of IBMB that work for a variety of GNNs and datasets. They substantially
 59 accelerate inference and training without sacrificing accuracy, especially for small label ratios.
- 60 • Methods for mitigating the impact of fixed, local mini-batches and sparse gradients on training.

61 2 Background and related work

62 **Graph neural networks.** We consider a graph $\mathcal{G} = (\mathcal{V}, \mathcal{E})$ with node set \mathcal{V} and (possibly directed)
 63 edge set \mathcal{E} . $N = |\mathcal{V}|$ denotes the number of nodes, $E = |\mathcal{E}|$ the number of edges, and $\mathbf{A} \in \mathbb{R}^{N \times N}$
 64 the adjacency matrix. GNNs use one embedding per node $\mathbf{h}_u \in \mathbb{R}^H$ and edge $\mathbf{e}_{(uv)} \in \mathbb{R}^{H_e}$ of size H
 65 and H_e , and update them in each layer via message passing between neighboring nodes. We denote
 66 the embedding in layer l as $\mathbf{h}_u^{(l)}$ and its i 'th entry as $\mathbf{h}_{ui}^{(l)}$. Most GNNs can be expressed via the
 67 following equations:

$$\mathbf{h}_u^{(l+1)} = f_{\text{node}}(\mathbf{h}_u^{(l)}, \text{Agg}_{v \in \mathcal{N}_u} [f_{\text{msg}}(\mathbf{h}_u^{(l)}, \mathbf{h}_v^{(l)}, \mathbf{e}_{(uv)}^{(l)})]), \quad (1)$$

$$\mathbf{e}_{(uv)}^{(l+1)} = f_{\text{edge}}(\mathbf{h}_u^{(l+1)}, \mathbf{h}_v^{(l+1)}, \mathbf{e}_{(uv)}^{(l)}). \quad (2)$$

68 The node and edge update functions f_{node} and f_{edge} , and the message function f_{msg} can be imple-
 69 mented using e.g. linear layers, multi-layer perceptrons (MLPs), and skip connections. The node's
 70 neighborhood \mathcal{N}_u is usually defined directly by the graph \mathcal{G} [27], but can be generalized to consider
 71 larger or even global neighborhoods [1, 16], or feature similarity [10]. The most common aggregation
 72 function Agg is summation, but multiple other alternatives have also been explored [9, 17]. Edge
 73 embeddings $\mathbf{e}_{(uv)}$ are often not used in GNNs, but some variants rely on them exclusively [6].

74 **Scalable GNNs.** Multiple works have proposed massively scalable GNNs that leverage the
 75 peculiarities of message passing to condense it into a single step, akin to label or feature propagation
 76 [4, 14]. Our work focuses on general, model-agnostic scalability methods.

77 **Scalable graph learning.** Classical graph learning faced issues similar to GNNs when scaling to
 78 large graphs. Multiple frameworks for distributed graph computations were proposed to solve this
 79 without approximations or sampling [19, 28, 31, 32]. Other works scaled to large graphs via stochastic
 80 variational inference, e.g. by sampling nodes and node pairs [20]. Interestingly, this approach is quite
 81 similar to sampling-based mini-batching for GNNs.

82 **Mini batching for GNNs.** Previous mini-batching methods can largely be divided into three
 83 categories: Node-wise sampling, layer-wise sampling, and subgraph-based sampling [29]. In node-
 84 wise sampling, we obtain a separate set of auxiliary nodes for every output node, which are sampled
 85 independently for each message passing step. Each output node is treated independently; if two output
 86 nodes sample the same auxiliary node, we compute its embedding twice [21, 30, 39]. Layer-wise
 87 sampling jointly considers all output nodes of a batch to compute a stochastic set of activations in
 88 each layer. Computations on auxiliary nodes are thus shared [5, 23, 42]. Subgraph-based sampling
 89 selects a meaningful subgraph and then runs the GNN on this subgraph as if it were the full graph.
 90 This method thus computes the outputs and intermediate embeddings of all nodes in that subgraph

¹<https://figshare.com/s/f615b330391677014bc5>

91 [7, 40]. Our method most closely resembles the subgraph-based sampling approach. However, IBMB
 92 considers both output and auxiliary nodes, resulting in better batches, and only computes the output
 93 of predetermined output nodes, similar to node-wise sampling. Note that mini-batch generation is an
 94 orthogonal problem to training frameworks such as GNNAutoScale [13]. We can also use IBMB to
 95 provide mini-batches as part of GNNAutoScale.

96 3 Influence-based mini-batching

97 **Influence scores.** To effectively create graph-based mini-batches we must first quantify how important
 98 one node is for another node’s prediction. As proposed by Xu et al. [38], we can do this via the
 99 influence score, which determines the local sensitivity of the output at node u on the input at node v as:

$$I(v, u) = \sum_i \sum_j \left| \frac{\partial \mathbf{h}_{ui}^{(L)}}{\partial \mathbf{X}_{vj}} \right|, \quad (3)$$

100 where $\mathbf{h}_{ui}^{(L)}$ is the i ’th entry in the embedding of node u in the last layer L and \mathbf{X}_{vj} is feature j of
 101 node v . Analyzing the expected influence score can provide a crisp understanding of how to select
 102 nodes for inference when we only have knowledge of the graph, not the model or the node features.
 103 To formally prove this connection, we consider a slightly limited class of GNNs and model our lack
 104 of knowledge via a randomization assumption of ReLU activations, similar to Choromanska et al.
 105 [8], and by assuming that all nodes have the same expected features, yielding (proof in App. A):

106 **Theorem 1.** *Given a GNN with linear, graph-dependent aggregation and ReLU activations. Assume
 107 that all paths in the model’s computation graph are activated with the same probability ρ and nodes
 108 have features with expected value $\mathbb{E}[X_{v,i}] = \chi_i$. If we restrict the model input features to a set of
 109 auxiliary nodes $\mathcal{S}_{\text{aux}} \subseteq \mathcal{V}$, then the error*

$$\|\tilde{\mathbf{h}}_u^{(L)} - \mathbf{h}_u^{(L)}\|_1 \quad (4)$$

110 *between the approximate logits $\tilde{\mathbf{h}}_u^{(L)}$ and the true logits $\mathbf{h}_u^{(L)}$ is minimized, in expectation, by selecting
 111 the nodes $v \in \mathcal{S}_{\text{aux}}$ with maximum influence score $I(v, u)$.*

112 **Formalizing mini-batching.** We can leverage this insight by formalizing the mini-batching as the
 113 optimization problem

$$\underbrace{\max_{\substack{P_{\text{out}} \in \mathbb{P}(\mathcal{V}_{\text{out}}) \\ |P_{\text{out}}|=b}} \sum_{\mathcal{S}_{\text{out}} \in P_{\text{out}}}}}_{\text{Output node partitioning}} \underbrace{\max_{\substack{\mathcal{S}_{\text{aux}} \subseteq \mathcal{V} \\ |\mathcal{S}_{\text{aux}}| \leq B}} \sum_{u \in \mathcal{S}_{\text{out}}} \sum_{v \in \mathcal{S}_{\text{aux}}}}}_{\text{Auxiliary node selection}} \underbrace{I(v, u)}_{\text{Influence score}}, \quad (5)$$

114 where $\mathbb{P}(\mathcal{V}_{\text{out}})$ denotes the set of partitions of the output nodes \mathcal{V}_{out} , b the number of batches, and B
 115 the maximum batch size. This optimization yields two results: The output node partition P_{out} and the
 116 auxiliary node set for each batch of output nodes, \mathcal{S}_{aux} . The hyperparameter B is determined by the
 117 available (GPU) memory, while b trades off runtime and approximation quality. This formulation
 118 optimizes the average approximation across all outputs. This might not be ideal since some nodes
 119 might already be approximated well with a lower number of auxiliary nodes. We can instead focus
 120 on the worst-case approximation by optimizing the minimum aggregate influence score as

$$\underbrace{\max_{\substack{P_{\text{out}} \in \mathbb{P}(\mathcal{V}_{\text{out}}) \\ |P_{\text{out}}|=b}} \min_{\mathcal{S}_{\text{out}} \in P_{\text{out}}}}}_{\text{Output node partitioning}} \underbrace{\max_{\substack{\mathcal{S}_{\text{aux}} \subseteq \mathcal{V} \\ |\mathcal{S}_{\text{aux}}| \leq B}} \min_{u \in \mathcal{S}_{\text{out}}} \sum_{v \in \mathcal{S}_{\text{aux}}}}}_{\text{Auxiliary node selection}} \underbrace{I(v, u)}_{\text{Influence score}}. \quad (6)$$

121 Both Eqs. (5) and (6) split the mini-batching problem into three parts: Output node partitioning,
 122 auxiliary node selection, and influence score computation. We call this approach influence-based
 123 mini-batching (IBMB).

124 **Computing influence scores.** The model’s influence score depends on various model details,
 125 especially when considering exact, trained models. In many cases we can calculate the expected
 126 influence score by making simplifying assumptions, similar to Theorem 1. This allows tailoring the
 127 mini-batching method to the exact model of interest. For the remainder of this work we will focus
 128 our analysis on the broad class of models that use the average as an aggregation function, such as

129 graph convolutional networks (GCN) [27]. In this case, we can make similar assumptions on the
 130 GNN as in [Theorem 1](#) to prove that the influence score is proportional to a slightly modified random
 131 walk with L steps [38]. To remove the influence score’s dependence on the number of layers L , we
 132 can furthermore take the limit $L \rightarrow \infty$. Unfortunately, this would result in a limit distribution that
 133 is independent of node v . To avoid this we add restarts to the random walk, as proposed by Gasteiger
 134 et al. [15]. The limit $L \rightarrow \infty$ then becomes equivalent to personalized PageRank (PPR), which we
 135 can thus use an approximation of the influence score. Notably, PPR even works well for models with
 136 more complex, data-dependent influence scores, such as GAT (see [Sec. 5](#)). The PPR matrix is given by

$$\mathbf{\Pi}^{\text{PPR}} = \alpha(\mathbf{I}_N - (1 - \alpha)\mathbf{D}^{-1}\mathbf{A})^{-1}, \quad (7)$$

137 with the teleport probability $\alpha \in (0, 1]$ and the diagonal degree matrix $D_{ii} = \sum_k A_{ik}$. The entry
 138 Π_{uv}^{PPR} then provides a measure for the influence of node v on u . Calculating the above inverse is
 139 obviously infeasible for large graphs. However, we can approximate $\mathbf{\Pi}^{\text{PPR}}$ with a sparse matrix $\tilde{\mathbf{\Pi}}^{\text{PPR}}$
 140 in time $\mathcal{O}(\frac{1}{\varepsilon\alpha})$ per row, with error $\varepsilon \deg(v)$ [2]. Importantly, this approximation uses only the node’s
 141 local neighborhood, making its runtime independent of the overall graph size and thus massively
 142 scalable. Furthermore, the calculation is deterministic and model-independent, so we only need to
 143 perform this computation once during preprocessing.

144 3.1 Auxiliary node selection

145 **Node-wise selection.** Selecting auxiliary nodes on large graphs requires a method that efficiently
 146 yields nodes with highest expected influence. Fortunately, there is a well-developed literature of
 147 methods for finding the top-k PPR nodes. The classic approximate PPR method [2] is guaranteed
 148 to provide all nodes with a PPR value $\Pi_{uv}^{\text{PPR}} > \varepsilon \deg(v)$ w.r.t. the root (output) node u . Optimizing
 149 auxiliary nodes by the worst-case influence score ([Eq. \(6\)](#)) thus equates to separately running
 150 approximate PPR for each output node in a batch \mathcal{S}_{out} , and then merging them.

151 **Batch-wise selection.** Considering each output node separately does not take into account how one
 152 auxiliary node jointly affects multiple output nodes, as required for the average-case formulation
 153 in [Eq. \(5\)](#). Fortunately, PPR calculation can be adapted to use a set of root nodes. To do so, we
 154 use a set of nodes in the teleport vector \mathbf{t} instead of a single node, e.g. by leveraging the underlying
 155 recursive equation for a PPR vector $\pi_{\text{ppr}}(\mathbf{t}) = (1 - \alpha)\mathbf{D}^{-1}\mathbf{A}\pi_{\text{ppr}}(\mathbf{t}) + \alpha\mathbf{t}$. \mathbf{t} is a one-hot vector in
 156 the node-wise setting, while for batch-wise PPR it is $1/|\mathcal{S}_{\text{out}}|$ for all nodes in \mathcal{S}_{out} . This variant is
 157 also known as topic-sensitive PageRank. We found that batch-wise PPR is significantly faster than
 158 node-wise PPR. However, it can lead to cases where one outlier node receives almost no neighbors,
 159 while others have excessively many. Whether node-wise or batch-wise selection performs better thus
 160 often depends on the dataset and model.

161 **Subgraph generation.** Creating mini-batches also requires selecting a subgraph of relevant edges.
 162 We do so by using the subgraph induced by the selected output and auxiliary nodes in a batch. Note
 163 that the above node selection methods ignore how these changes to the graph affect the influence
 164 scores. This is a limitation of these methods. However, PPR is a *local clustering* method and we can
 165 thus expect auxiliary nodes to be well-connected.

166 3.2 Output node partitioning

167 **Optimal partitioning.** Finding the optimal node partition in [Eqs. \(5\) and \(6\)](#) would require trying out
 168 every possible partition since a change in \mathcal{S}_{out} can unpredictably affect the optimal choice of auxiliary
 169 nodes. Doing so is clearly intractable since the number of partitions grows exponentially with N for
 170 a fixed batch size. We thus need to approximate the optimal partition via a scalable heuristic. The
 171 implicit goal of this step is finding output nodes that share a large number of auxiliary nodes. One
 172 good proxy for these overlaps is the proximity of nodes in the graph.

173 **Distance-based partitioning.** We propose two methods that leverage graph locality as a heuristic.
 174 The first is based on node distances. In this approach we first compute the pairwise node distances
 175 between nodes that are close in the graph. We can use PPR for this as well, since it is also commonly
 176 used as a node distance. If we select auxiliary nodes with node-wise PPR, we thus only need to
 177 calculate PPR scores once for both steps.

178 Next, we greedily construct the partition P_{out} from $\tilde{\mathbf{\Pi}}^{\text{PPR}}$. To do so, we start by putting every node u
 179 into a separate batch $\{u\}$. We then sort all elements in $\tilde{\mathbf{\Pi}}^{\text{PPR}}$ by magnitude, independent of their row

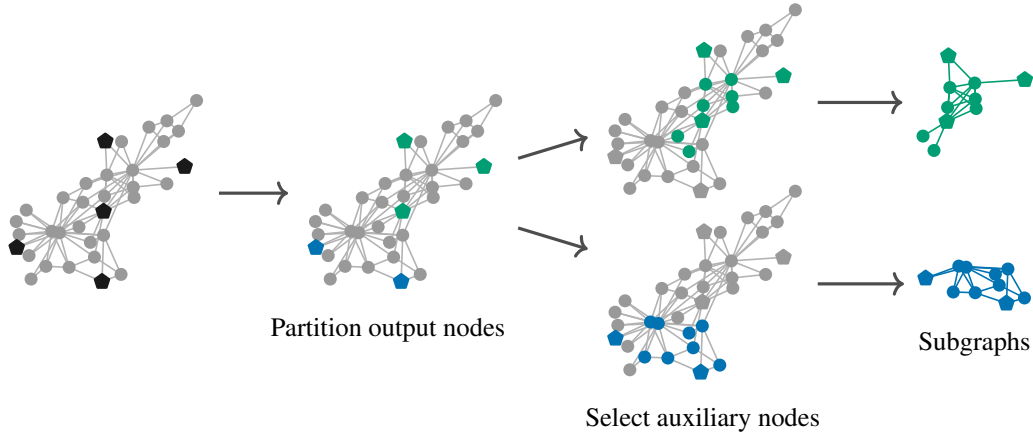


Figure 1: Practical example of influence-based mini-batching (IBMB). The output nodes are indicated by pentagons. These nodes are first partitioned into batches, e.g. by grouping nearby nodes together. We then use influence scores to select the auxiliary nodes of each batch, e.g. neighbors with top- k personalized PageRank (PPR) scores. Finally, we generate a batch using the induced subgraph of all selected nodes, but only calculate the outputs of the output nodes we chose when partitioning. Batches can overlap and do not need to cover the whole graph.

180 or column. We scan over these values in descending order, considering the value’s indices (u, v) and
 181 merging the batches containing the two nodes. Afterwards we randomly merge any small leftover
 182 batches. We stay within memory constraints by only merging batches that stay below the maximum
 183 batch size B . This method achieves well-overlapping batches and can efficiently add incrementally
 184 incoming out nodes, e.g. in a streaming setting. Our experiments show that this method achieves a
 185 good compromise between well-overlapping batches and good gradients for training (see Sec. 5).
 186 Note that the resulting partition is unbalanced, i.e. some sets will be larger than others.

187 **Graph partitioning.** For our second method, we note that partitioning output nodes into overlapping
 188 mini-batches is closely related to partitioning graphs. We can thus leverage the extensive research on
 189 this topic by using the METIS graph partitioning algorithm [25] to find a partition of output nodes
 190 P_{out} . We found that graph partitioning yields roughly a two times higher overlap of auxiliary nodes
 191 than distance-based partitioning, thus leading to significantly more efficient batches. However, it also
 192 results in worse gradient samples, which we found to be detrimental for training (see Sec. 5). Note
 193 that Cluster-GCN also uses graph partitioning, and thus aligns somewhat with the IBMB framework
 194 [7]. However, IBMB additionally selects relevant auxiliary nodes and ignores irrelevant parts of the
 195 graph. This significantly accelerates training on small training sets and improves the accuracy of
 196 output nodes close to the partition boundary.

197 **Computational complexity.** Since IBMB ignores irrelevant parts of the graph, inference and training
 198 scale linearly in the number of output nodes $\mathcal{O}(N_{\text{out}})$. Preprocessing runs in $\mathcal{O}(\frac{N_{\text{out}}}{\epsilon\alpha})$ for node-wise
 199 PPR-based steps, $\mathcal{O}(\frac{b}{\epsilon\alpha})$ for batch-wise PPR, and in $\mathcal{O}(E)$ for graph partitioning. The runtime of
 200 IBMB is thus *independent* of the graph size if we use distance-based partitioning. Fig. 1 gives an
 201 overview of the full practical IBMB process.

202 4 Training with IBMB

203 **Computational advantages.** The above analysis focused on node outputs, not gradient estimation and
 204 training. However, IBMB also has inherent advantages for training, since we need to perform mini-
 205 batch generation only once during preprocessing. We can then cache each mini-batch in consecutive
 206 blocks of memory, thereby allowing the data to be stored where it is needed and circumventing
 207 expensive random data accesses. This significantly accelerates training, allows efficient distributed
 208 training, and enables more expensive node selection procedures. In contrast, most previous methods
 209 select both output and auxiliary nodes randomly in each epoch, which incurs significant overhead.

210 Our experiments show that IBMB’s more efficient memory accesses clearly outweigh the slightly
 211 worse gradient estimates (see Sec. 5). This seems counter-intuitive since the deterministic, fixed
 212 mini-batches in IBMB only provide sparse, fixed gradient samples. In this section we discuss these
 213 aspects and how adaptive optimization and batch scheduling counteract their effects.

214 **Sparse gradients.** Partitioning output nodes based on proximity effectively correlates the gradients
 215 sampled in a batch. The model thus sees a sparse gradient sample, which does not cover all aspects of
 216 the dataset. Fortunately, adaptive optimization methods such as Adagrad and Adam were developed
 217 exactly for such sparse gradients [12, 26]. We furthermore ensure an unbiased training process by
 218 using every output (training) node exactly once per epoch.

219 **Fixed batches.** Using a *fixed* set of batches can lead to problems with basic stochastic gradient
 220 descend (SGD) as well. Imagine training with two fixed batches whose loss functions have different
 221 minima. If training has “converged” to one of these minima, SGD would start to oscillate: It
 222 would take one step towards the other minimum, and then back, and so forth. To counteract this
 223 oscillation, we could add a “consensus constraint” to enforce a consensus between the weights
 224 after different batches, akin to distributed optimization [33]. We can solve this constraint using a
 225 primal-dual saddle-point algorithm with directed communication [18]. The resulting dynamics are
 226 $\dot{x}^{(t)} = -\nabla \tilde{f}^{(t)}(x^{(t)}) - \alpha \lambda \dot{x}^{(t-1)} - \lambda^2 \dot{x}^{(t-2)}$, with the weights $x^{(t)}$ at time step t , the learning rate
 227 λ and the dual variable α . These dynamics resemble SGD with momentum, and fit perfectly into
 228 the framework of adaptive optimization methods [34]. Indeed, momentum and adaptive methods
 229 suppress the oscillations in the above example with two minima. Accordingly, prior works have
 230 also found benefits in deterministically selecting fixed mini-batches [3, 37]. We further improve
 231 convergence by adaptively reducing the learning rate when the validation loss plateaus, which ensures
 232 that the step size decreases consistently.

233 **Batch scheduling.** While Adam with learning rate scheduling consistently ensures convergence,
 234 we still observe downward spikes in accuracy during training. To illustrate this issue, consider a
 235 sequence of mini-batches. In regular training every mini-batch is similar and the order of these
 236 batches is irrelevant. In our case, however, some of the mini-batches might be very similar. If
 237 the optimizer sees a series of similar batches, it will take increasingly large steps in a suboptimal
 238 direction, which leads to the observed downward spikes in accuracy. We propose to prevent these
 239 suboptimal batch sequences by optimizing the order of batches. To quantify batch similarity we
 240 measure the symmetrized KL-divergence of the label distribution between batches. In particular, we
 241 use the normalized training label distribution $p_i = c_i / \sum_j c_j$, where c_i is the number of training
 242 nodes of class i . This results in the pairwise batch distance d_{ab} between batches a and b . We propose
 243 two ways to use this for improving the batch schedule: (i) Find the fixed batch cycle that *maximizes*
 244 the batch distances between consecutive batches. This is a traveling salesman problem for finding
 245 the maximum distance loop that visits all batches. It is therefore only feasible for a small number of
 246 batches. (ii) Sample the next batch weighted by the distance to the current batch. Both scheduling
 247 methods improve convergence and increase final accuracy, at almost no cost during training. Overall,
 248 our training scheme leads to consistent convergence. Even accumulating gradients over the whole
 249 epoch does not significantly change convergence or final accuracy (see Fig. 8).

250 5 Experiments

251 **Experimental setup.** We show results for two variants of our method: IBMB with PPR
 252 distance-based batches and node-wise PPR clustering (node-wise IBMB), and IBMB with graph
 253 partition-based batches and batch-wise PPR clustering (batch-wise IBMB). We also experimented
 254 with the two other combinations of the output node partitioning and auxiliary node selection variants,
 255 but found these two to work best. We compare them to four state-of-the-art mini-batching methods:
 256 Neighbor sampling [21], Layer-Dependent Importance Sampling (LADIES) [42], GraphSAINT-RW
 257 [40], shaDow [41], and Cluster-GCN [7]. We use four large node classification datasets for
 258 evaluation: ogbn-arxiv [22, 36, ODC-BY], ogbn-products [36, Amazon license], Reddit [21], and
 259 ogbn-papers100M [22, 36, ODC-BY]. While these datasets use the transductive setting, IBMB makes
 260 no assumptions about this and can equally be applied to the inductive setting. We skip the common,
 261 small datasets (Cora, Citeseer, PubMed) since they are ill-suited for evaluating scalability methods.
 262 We do not strive to set a new accuracy record but instead aim for a consistent, fair comparison based
 263 on three standard GNNs: GCN [27], graph attention networks (GAT) [35], and GraphSAGE [21]. We
 264 use the same training pipeline for all methods, giving them access to the same optimizations. Since

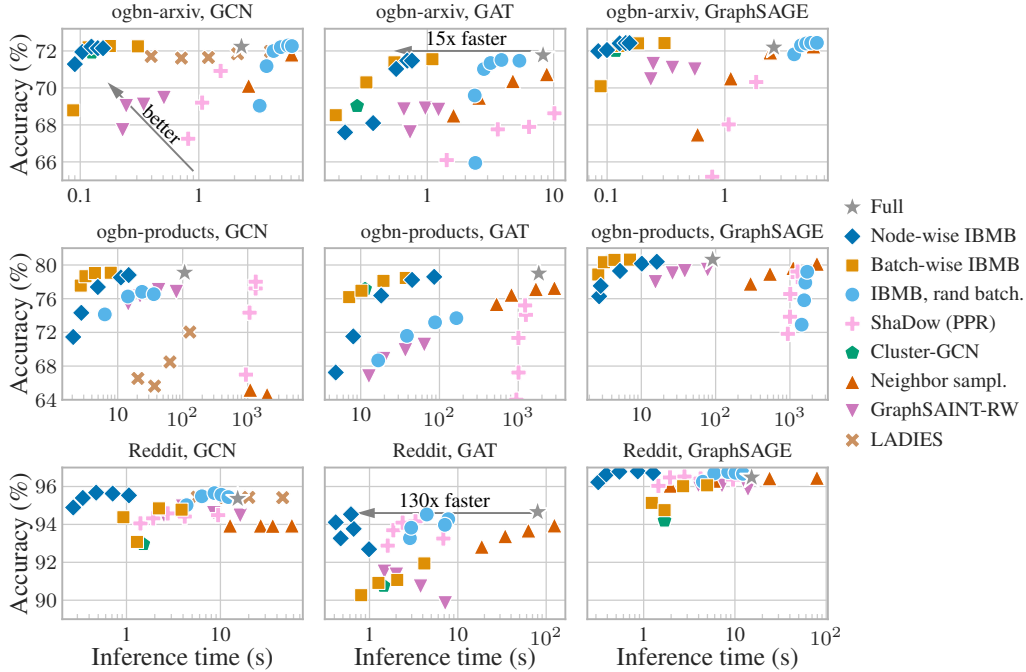


Figure 2: Test accuracy and log. inference time averaged over a fixed set of 10 pretrained GNNs. IBMB provides the best accuracy versus time trade-off (top-left corner) in all settings.

265 full inference is too slow to execute every epoch we use the mini-batching method used for training
 266 to also approximate inference during training. We run each experiment 10 times and report the
 267 mean and standard deviation in all tables and the bootstrapped mean and 95 % confidence intervals
 268 in all figures. We fully pipeline data loading and batch creation by prefetching batches in parallel.
 269 We found that using more than one worker for this does not improve runtime, most likely because
 270 data loading is limited by the memory bandwidth, which is shared between workers. We keep GPU
 271 memory usage constant between methods, and tune all remaining hyperparameters for both IBMB
 272 and the baselines. See App. B for full experimental details.

273 **Inference.** Fig. 2 compares inference accuracy and time of different batching methods, using the same
 274 pretrained model and varying computational budgets (number of auxiliary nodes/sampled nodes) at
 275 a fixed GPU memory budget. IBMB provides the best trade-off between accuracy and time in all set-
 276 tings. Node-wise IBMB performs better than graph partitioning, except on ogbn-products. IBMB pro-
 277 vides a significant speedup over chunking-based full-batch inference on GPU, being 10 to 900 times
 278 faster at comparable accuracy. All previous methods are either significantly slower or less accurate.

279 **Training.** IBMB performs significantly better in training than previous methods, converging up to
 280 17x faster than all baselines (see Fig. 3). This is *despite* the fact that we always prefetch the next batch
 281 in parallel. Note that GAT is slower to compute than GCN and GraphSAGE, limiting the positive
 282 impact of a fast batching method. Compute-constrained models like GAT are less relevant in practice
 283 since data access is typically the bottleneck for GNNs on large, often even disk-based datasets [4].
 284 Table 7 in the appendix furthermore shows that IBMB’s time per epoch is significantly faster than
 285 all sampling-based methods. Cluster-GCN has a comparable runtime, which is expected due to its
 286 similarity with IBMB. However, it converges more slowly than IBMB and reaches substantially lower
 287 final accuracy. Neighbor sampling achieves good final accuracy, but is extremely slow. GraphSAINT-
 288 RW only achieves good final accuracy with prohibitively expensive full-batch inference. Node-wise
 289 IBMB achieves the best final accuracy with a scalable inference method in 7 out of 10 settings. On
 290 ogbn-papers100M, IBMB has a substantially faster time per epoch and lower memory consumption
 291 than previous methods demonstrating IBMB’s favorable scaling with dataset size. It even performs
 292 as well as SIGN-XL ((66.1±0.2) %) [14], while using 30x fewer parameters and no hyperparameter
 293 tuning. Notably, we were unable to evaluate GraphSAINT-RW and Cluster-GCN on this dataset,
 294 since they use more than 256 GB of main memory.

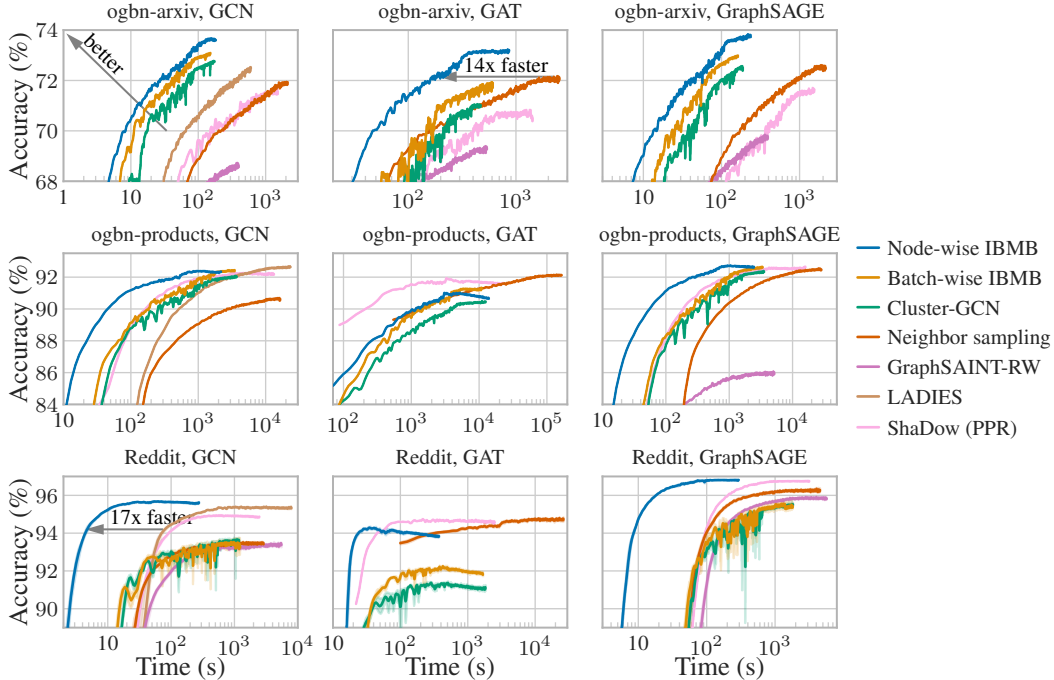


Figure 3: Training convergence of validation accuracy in log. time. Average and 95 % confidence interval of 10 runs. GraphSAINT-RW does not reach the shown accuracy range in some settings due to its bad validation performance. IBMB converges the fastest in 9 out of 10 settings.

295 **Preprocessing.** IBMB requires more preprocessing than previous methods. However, since IBMB
 296 is rather insensitive to hyperparameter choices (see Fig. 5, Table 5), preprocessing rarely needs to
 297 be re-run. Instead, its result can be saved to disk and re-used for training different models. Just
 298 considering our 10 training seeds, preprocessing of node-wise IBMB only took 1.3 % of the training
 299 time for GCN and 0.25 % for GAT on ogbn-arxiv.

300 **Training set size.** The ogbn-arxiv and ogbn-products datasets both contain a large number of
 301 training nodes (91k and 197k, respectively). However, labeling training samples is often an expensive
 302 endeavor, and models are commonly trained with only a few hundred or thousand training samples.
 303 GraphSAINT-RW and Cluster-GCN are global training methods, i.e. they always use the whole graph
 304 for training. They are thus ill-suited for the common setting of a large overall graph containing a
 305 small number of training nodes (resulting in a small label rate). In contrast, the training time of
 306 IBMB purely scales with the number of training nodes. To demonstrate this, we reduce the label rate
 307 by sub-sampling the training nodes of ogbn-products and compare the convergence in Fig. 4. As
 308 expected, the gap in convergence speed between IBMB and both Cluster-GCN and GraphSAINT-RW
 309 grows even larger for smaller training sets.

310 **Ablation studies.** We ablate our output node partitioning schemes by instead batching together
 311 random sets of nodes. We use fixed batches since we found that resampling incurs significant
 312 overhead without benefits – which is consistent with our considerations on gradient samples and
 313 contiguous memory accesses. Fig. 6 shows that this method (“Fixed random”) converges more
 314 slowly and does not reach the same level of accuracy as our partition schemes. Node-wise IBMB
 315 converges the fastest, which suggests a trade-off between full gradient samples (random batching)
 316 and maximum batch overlap (graph partitioning). Fig. 2 shows that random batching (“IBMB, rand
 317 batch.”) is also substantially slower and often less accurate for inference. This is due to the synergy
 318 effects of output node partitioning: If output nodes have similar auxiliary nodes, they benefit from
 319 each other’s neighborhood. We ablate auxiliary node selection by comparing IBMB to Cluster-GCN,
 320 since it just uses the graph partition as a batch instead of smartly selecting auxiliary nodes. We use
 321 the graph partition size as the number of auxiliary nodes for batch-wise IBMB to allow for a direct
 322 comparison. As discussed above, Cluster-GCN consistently performs worse, especially in terms of

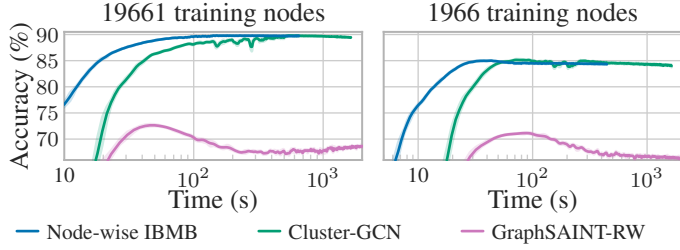


Figure 4: Training convergence in log. time for GCN on ogbn-products with smaller training sets. The gap in convergence speed between IBMB and the baselines grows larger for small training sets, since IBMB scales with training set size and not with overall graph size.

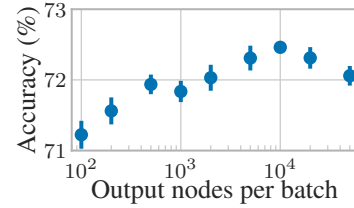


Figure 5: Trained accuracy for node-wise IBMB, depending on the output nodes per batch (GCN, ogbn-arxiv). The impact of this choice is rather minor.

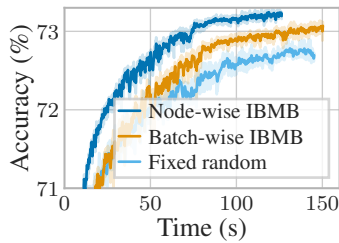


Figure 6: Convergence per time for training GCN on ogbn-arxiv. Both batch-wise and node-wise IBMB lead to faster convergence than fixed random batches.

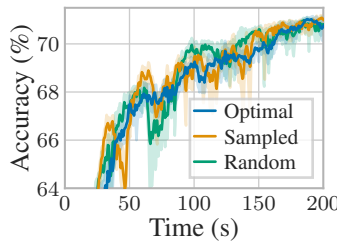


Figure 7: Batch scheduling for GAT on ogbn-arxiv. Optimal and weighted sampling-based scheduling improve convergence and prevent or reduce downward spikes in accuracy.

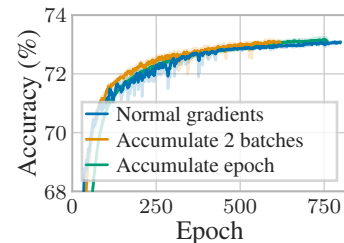


Figure 8: Gradient accumulation for batch-wise IBMB on GCN, ogbn-arxiv. The difference is minor, even when accumulating over the full epoch.

323 final accuracy, for inference, and for small label rates. Finally, Fig. 7 compares the proposed batch
 324 scheduling methods. Optimal and weighted sampling-based scheduling improve convergence and
 325 prevent or reduce downward spikes in accuracy.

326 **Sensitivity analysis.** Different IBMB is largely insensitive to different local clustering methods and
 327 hyperparameters for selecting auxiliary nodes (see Table 5). Even increasing the number of output
 328 nodes per batch with a fixed number of auxiliary nodes per output node only has a minor impact on
 329 accuracy, especially above 1000 output nodes per batch, as shown by Fig. 5. IBMB performs well even
 330 in extremely constrained settings with small batches of 100 output nodes per batch. In practice, IBMB
 331 only has one free hyperparameter: The number of auxiliary nodes per output node, which allows
 332 optimizing for accuracy or speed. The number of output nodes per batch is then given by the available
 333 GPU memory, while the local clustering method and other hyperparameters are not important.

334 **Gradient accumulation.** Accumulating gradients across multiple batches is a method for smoothing
 335 batches if gradient noise is too high. We might expect this to happen in IBMB due to the sparse
 336 gradients caused by primary node partitioning. However, Fig. 8 shows that gradient accumulation in
 337 fact only has an insignificant effect on IBMB, demonstrating its stability during training.

338 6 Conclusion

339 We propose influence-based mini-batching (IBMB), a method for extracting batches for GNNs.
 340 IBMB formalizes creating batches for inference by maximizing the influence score on the output
 341 nodes. Remarkably, with an adaptive optimizer and batch scheduling IBMB even performs well
 342 during training. It improves training convergence by up to 17x and inference time by up to 130x
 343 compared to previous methods that reach similar accuracy. IBMB performs especially well for sparse
 344 labels, large datasets, and when the pipeline is constrained by data access speed.

References

- 345
- 346 [1] Uri Alon and Eran Yahav. On the Bottleneck of Graph Neural Networks and its Practical
347 Implications. In *ICLR*, 2021. 2
- 348 [2] R. Andersen, F. Chung, and K. Lang. Local Graph Partitioning using PageRank Vectors. In
349 *FOCS*, 2006. 4, 14
- 350 [3] Subhankar Banerjee and Shayok Chakraborty. Deterministic Mini-batch Sequencing for Train-
351 ing Deep Neural Networks. In *AAAI*, 2021. 6
- 352 [4] Aleksandar Bojchevski, Johannes Gasteiger, Bryan Perozzi, Amol Kapoor, Martin Blais,
353 Benedek Rózemerczki, Michal Lukasik, and Stephan Günnemann. Scaling Graph Neural
354 Networks with Approximate PageRank. In *KDD*, 2020. 2, 7
- 355 [5] Jie Chen, Tengfei Ma, and Cao Xiao. FastGCN: Fast Learning with Graph Convolutional
356 Networks via Importance Sampling. In *ICLR*, 2018. 2
- 357 [6] Zhengdao Chen, Lisha Li, and Joan Bruna. Supervised Community Detection with Line Graph
358 Neural Networks. In *ICLR*, 2019. 2
- 359 [7] Wei-Lin Chiang, Xuanqing Liu, Si Si, Yang Li, Samy Bengio, and Cho-Jui Hsieh. Cluster-GCN:
360 An Efficient Algorithm for Training Deep and Large Graph Convolutional Networks. In *KDD*,
361 2019. 1, 3, 5, 6
- 362 [8] Anna Choromanska, Yann LeCun, and Gérard Ben Arous. Open Problem: The landscape of the
363 loss surfaces of multilayer networks. In *COLT*, 2015. 3, 12
- 364 [9] Gabriele Corso, Luca Cavalleri, Dominique Beaini, Pietro Liò, and Petar Veličković. Principal
365 Neighbourhood Aggregation for Graph Nets. In *NeurIPS*, 2020. 2
- 366 [10] Chenhui Deng, Zhiqiang Zhao, Yongyu Wang, Zhiru Zhang, and Zhuo Feng. GraphZoom: A
367 Multi-level Spectral Approach for Accurate and Scalable Graph Embedding. In *ICLR*, 2020. 2
- 368 [11] Johann Dréo, Alain Pérowski, Patrick Siarry, and Eric Taillard. *Metaheuristics for Hard*
369 *Optimization: Methods and Case Studies*. 2006. 13
- 370 [12] John C. Duchi, Elad Hazan, and Yoram Singer. Adaptive Subgradient Methods for Online
371 Learning and Stochastic Optimization. *Journal of Machine Learning Research*, 12:2121–2159,
372 2011. 6
- 373 [13] Matthias Fey, Jan E. Lenssen, Frank Weichert, and Jure Leskovec. GNNAutoScale: Scalable
374 and Expressive Graph Neural Networks via Historical Embeddings. In *ICML*, 2021. 3
- 375 [14] Fabrizio Frasca, Emanuele Rossi, Davide Eynard, Ben Chamberlain, Michael Bronstein, and
376 Federico Monti. SIGN: Scalable Inception Graph Neural Networks. *arXiv*, 2004.11198, 2020.
377 2, 7
- 378 [15] Johannes Gasteiger, Aleksandar Bojchevski, and Stephan Günnemann. Predict then Propagate:
379 Graph Neural Networks Meet Personalized PageRank. In *ICLR*, 2019. 4
- 380 [16] Johannes Gasteiger, Stefan Weißenberger, and Stephan Günnemann. Diffusion Improves Graph
381 Learning. In *NeurIPS*, 2019. 2
- 382 [17] Simon Geisler, Daniel Zügner, and Stephan Günnemann. Reliable Graph Neural Networks via
383 Robust Aggregation. In *NeurIPS*, 2020. 2
- 384 [18] Bahman Ghahesifard and Jorge Cortés. Distributed Continuous-Time Convex Optimization on
385 Weight-Balanced Digraphs. *IEEE Transactions on Automatic Control*, 59(3):781–786, 2014. 6
- 386 [19] Joseph E. Gonzalez, Yucheng Low, Haijie Gu, Danny Bickson, and Carlos Guestrin. Power-
387 Graph: Distributed Graph-Parallel Computation on Natural Graphs. In *OSDI*, 2012. 2
- 388 [20] Prem K. Gopalan, Sean Gerrish, Michael Freedman, David Blei, and David Mimno. Scalable
389 Inference of Overlapping Communities. In *NeurIPS*, 2012. 2
- 390 [21] William L. Hamilton, Zhitao Ying, and Jure Leskovec. Inductive Representation Learning on
391 Large Graphs. In *NeurIPS*, 2017. 1, 2, 6
- 392 [22] Weihua Hu, Matthias Fey, Marinka Zitnik, Yuxiao Dong, Hongyu Ren, Bowen Liu, Michele
393 Catasta, and Jure Leskovec. Open Graph Benchmark: Datasets for Machine Learning on Graphs.
394 In *NeurIPS*, 2020. 6

- 395 [23] Wenbing Huang, Tong Zhang, Yu Rong, and Junzhou Huang. Adaptive Sampling Towards Fast
396 Graph Representation Learning. In *NeurIPS*, 2018. 2
- 397 [24] Gadi Hutt, Vibhav Viswanathan, and Adam Nadolski. Deliver high performance ML inference
398 with AWS Inferentia, 2019. 1
- 399 [25] George Karypis and Vipin Kumar. A Fast and High Quality Multilevel Scheme for Partitioning
400 Irregular Graphs. *SIAM Journal on Scientific Computing*, 20(1):359–392, 1998. 5
- 401 [26] Diederik P. Kingma and Jimmy Ba. Adam: A Method for Stochastic Optimization. In *ICLR*,
402 2015. 6
- 403 [27] Thomas N. Kipf and Max Welling. Semi-Supervised Classification with Graph Convolutional
404 Networks. In *ICLR*, 2017. 2, 4, 6
- 405 [28] Aapo Kyrola, Guy Blelloch, and Carlos Guestrin. GraphChi: Large-Scale Graph Computation
406 on Just a PC. In *OSDI*, 2012. 2
- 407 [29] Xin Liu, Mingyu Yan, Lei Deng, Guoqi Li, Xiaochun Ye, and Dongrui Fan. Sampling Methods
408 for Efficient Training of Graph Convolutional Networks: A Survey. *IEEE/CAA Journal of*
409 *Automatica Sinica*, 9(2):205–234, 2022. 2
- 410 [30] Ziqi Liu, Zhengwei Wu, Zhiqiang Zhang, Jun Zhou, Shuang Yang, Le Song, and Yuan Qi.
411 Bandit Samplers for Training Graph Neural Networks. In *NeurIPS*, 2020. 2
- 412 [31] Yucheng Low, Danny Bickson, Joseph Gonzalez, Carlos Guestrin, Aapo Kyrola, and Joseph M.
413 Hellerstein. Distributed GraphLab: a framework for machine learning and data mining in the
414 cloud. In *VLDB*, 2012. 2
- 415 [32] Grzegorz Malewicz, Matthew H. Austern, Aart J.C Bik, James C. Dehnert, Ilan Horn, Naty
416 Leiser, and Grzegorz Czajkowski. Pregel: a system for large-scale graph processing. In
417 *SIGMOD*, 2010. 2
- 418 [33] Reza Olfati-Saber, J. Alex Fax, and Richard M. Murray. Consensus and Cooperation in
419 Networked Multi-Agent Systems. *Proceedings of the IEEE*, 95(1):215–233, 2007. 6
- 420 [34] Sashank J. Reddi, Satyen Kale, and Sanjiv Kumar. On the Convergence of Adam and Beyond.
421 In *ICLR*, 2018. 6
- 422 [35] Petar Veličković, Guillem Cucurull, Arantxa Casanova, Adriana Romero, Pietro Liò, and Yoshua
423 Bengio. Graph Attention Networks. In *ICLR*, 2018. 6
- 424 [36] Kuansan Wang, Zhihong Shen, Chiyuan Huang, Chieh-Han Wu, Yuxiao Dong, and Anshul
425 Kanakia. Microsoft Academic Graph: When experts are not enough. *Quantitative Science*
426 *Studies*, 1(1):396–413, 2020. 6
- 427 [37] Shengjie Wang, Wenruo Bai, Chandrashekar Lavania, and Jeff Bilmes. Fixing Mini-batch
428 Sequences with Hierarchical Robust Partitioning. In *AISTATS*, 2019. 6
- 429 [38] Keyulu Xu, Chengtao Li, Yonglong Tian, Tomohiro Sonobe, Ken-ichi Kawarabayashi, and
430 Stefanie Jegelka. Representation Learning on Graphs with Jumping Knowledge Networks. In
431 *ICML*, 2018. 3, 4
- 432 [39] Rex Ying, Ruining He, Kaifeng Chen, Pong Eksombatchai, William L. Hamilton, and Jure
433 Leskovec. Graph Convolutional Neural Networks for Web-Scale Recommender Systems. In
434 *KDD*, 2018. 2
- 435 [40] Hanqing Zeng, Hongkuan Zhou, Ajitesh Srivastava, Rajgopal Kannan, and Viktor Prasanna.
436 GraphSAINT: Graph Sampling Based Inductive Learning Method. In *ICLR*, 2020. 3, 6
- 437 [41] Hanqing Zeng, Muhan Zhang, Yinglong Xia, Ajitesh Srivastava, Andrey Malevich, Rajgopal
438 Kannan, Viktor Prasanna, Long Jin, and Ren Chen. Decoupling the Depth and Scope of Graph
439 Neural Networks. In *NeurIPS*, 2021. 6
- 440 [42] Difan Zou, Ziniu Hu, Yewen Wang, Song Jiang, Yizhou Sun, and Quanquan Gu. Layer-
441 Dependent Importance Sampling for Training Deep and Large Graph Convolutional Networks.
442 In *NeurIPS*, 2019. 1, 2, 6

443 A Proof of Theorem 1

444 **Path-based view of neural networks.** We can view a neural network with ReLUs as a directed
 445 acyclic computational graph and express the i 'th output logit via paths through this graph as

$$\mathbf{h}_i^{(L)} = \frac{1}{\lambda^{(H-1)/2}} \sum_{q=1}^{\phi} Z_{i,q} X_{i,q} \prod_{l=1}^L w_{i,q}^{(l)}, \quad (8)$$

446 where λ is a constant related to the size of the network [8] and ϕ is the total number of paths.
 447 Furthermore, $Z_{(i,q)} \in \{0, 1\}$ denotes whether the path q is active or inactive when any ReLU is
 448 deactivated. $X_{(i,q)}$ represents the input feature used in the q -th path of logit i , and $w_{(i,q)}^{(l)}$ the used
 449 entry of the weight matrix W_l in layer l .

450 **Path-based view of GNNs.** We can extend this framework to graph neural networks by additionally
 451 introducing paths p through the (data-based) graph, starting from the auxiliary node v and ending at
 452 the output node u , as

$$\mathbf{h}_{u,i}^{(L)} = \frac{1}{\lambda^{(H-1)/2}} \sum_{v \in \mathcal{V}} \sum_{p=1}^{\psi} \sum_{q=1}^{\phi} Z_{v,p,i,q} X_{v,p,i,q} \prod_{l=1}^L a_{v,p}^{(l)} w_{i,q}^{(l)}, \quad (9)$$

453 where ψ is the total number of graph-based paths and $a_{v,p}^{(l)}$ denotes the graph-dependent but feature-
 454 independent aggregation weights. Note that $a_{v,p}^{(l)}$ depends on the whole path (v, p) and can thus be a
 455 function of any node and edge on this path, including the current and next layer's nodes.

456 **Expected influence score.** To obtain the influence score, we calculate the derivative

$$\frac{\partial \mathbf{h}_{u,i}^{(L)}}{\partial X_{v,j}} = \frac{1}{\lambda^{(H-1)/2}} \sum_{p=1}^{\psi} \sum_{q=1}^{\phi'} Z_{v,p,i,q} \prod_{l=1}^L a_{v,p}^{(l)} w_{i,q}^{(l)}, \quad (10)$$

457 with $X_{v,j}$ denoting input feature j at node v and ϕ' denoting the number of computational paths
 458 with input feature j . To simplify this expression, we use the assumption that all paths (v, p, i, q) are
 459 activated with the same probability ρ , i.e. $\mathbb{E}[Z_{v,p,i,q}] = \rho$, and compute the expectation:

$$\begin{aligned} \mathbb{E} \left[\frac{\partial \mathbf{h}_{u,i}^{(L)}}{\partial X_{v,j}} \right] &= \frac{1}{\lambda^{(H-1)/2}} \sum_{p=1}^{\psi} \sum_{q=1}^{\phi'} \rho \prod_{l=1}^L a_{v,p}^{(l)} w_{i,q}^{(l)} \\ &= \frac{\rho}{\lambda^{(H-1)/2}} \left(\sum_{p=1}^{\psi} \prod_{l=1}^L a_{v,p}^{(l)} \right) \left(\sum_{q=1}^{\phi'} \prod_{l=1}^L w_{i,q}^{(l)} \right). \end{aligned} \quad (11)$$

460 The only node-dependent term in the expected influence score $\mathbb{E}[I(v, u)] = \sum_i \sum_j \mathbb{E} \left[\left| \frac{\partial \mathbf{h}_{u,i}^{(L)}}{\partial X_{v,j}} \right| \right]$ is

461 thus $\left| \sum_{p=1}^{\psi} \prod_{l=1}^L a_{v,p}^{(l)} \right|$.

462 **Expected output.** We similarly obtain the expected output by additionally using the assumption that
 463 features have a node-independent expected value $\mathbb{E}[X_{v,p,i,q}] = \chi_{i,q}$, yielding

$$\begin{aligned} \mathbb{E}[\mathbf{h}_{u,i}^{(L)}] &= \frac{1}{\lambda^{(H-1)/2}} \sum_{v \in \mathcal{V}} \sum_{p=1}^{\psi} \sum_{q=1}^{\phi} \rho \chi_{i,q} \prod_{l=1}^L a_{v,p}^{(l)} w_{i,q}^{(l)} \\ &= \frac{\rho}{\lambda^{(H-1)/2}} \sum_{v \in \mathcal{V}} \left(\sum_{p=1}^{\psi} \prod_{l=1}^L a_{v,p}^{(l)} \right) \left(\sum_{q=1}^{\phi} \chi_{i,q} \prod_{l=1}^L w_{i,q}^{(l)} \right). \end{aligned} \quad (12)$$

464 Again, the only node-dependent term in the expected output is $\sum_{p=1}^{\psi} \prod_{l=1}^L a_{v,p}^{(l)}$. Adding any input
 465 node thus changes node u 's output in absolute terms by

$$\left| \sum_{p=1}^{\psi} \prod_{l=1}^L a_{v,p}^{(l)} \right| C = \mathbb{E}[I(v, u)] C', \quad (13)$$

466 with C and C' denoting all node-independent terms. Selecting the input nodes with maximum
 467 influence score $I(v, u)$ thus minimizes the L_1 norm of the approximation error. Note that this choice
 468 only considers the effect of selecting input nodes. It does not model the effect of changing the graph.

469 B Model and training details

470 **Hardware.** All experiments are run on an NVIDIA GeForce GTX 1080Ti. The experiments on ogbn-
 471 arxiv and ogbn-products use up to 64 GB of main memory. The experiments on ogbn-papers100M
 472 use up to 256 GB.

473 **Packages.** Our experiments are based on the following packages and versions:

- 474 • torch-geometric 1.7.0
- 475 – torch-cluster 1.5.9
- 476 – torch-scatter 2.0.6
- 477 – torch-sparse 0.6.9
- 478 • python 3.7.10
- 479 • ogb 1.3.1
- 480 • torch 1.8.1
- 481 • cudatoolkit 10.2.89
- 482 • numba 0.53.1
- 483 • python-tsp 0.2.0

484 **Preprocessing.** Before training, we first make the graph undirected, and add self-loops. The adjacency
 485 matrix is symmetrically normalized. We cache the symmetric adjacency matrix for graph partitioning
 486 and mini-batching. Instead of re-calculating the adjacency matrix normalization factors for GCN
 487 for each mini-batch, we re-use the global normalization factors. We found this to achieve similar
 488 accuracy at lower computational cost.

489 **Models.** We use three models for all the experiments: GCN (3 layers, hidden size 256 for the ogbn
 490 datasets and 2 layers, hidden size 512 for Reddit), GAT (3 layers, hidden size 128, 4 heads for the
 491 ogbn datasets and 2 layers, hidden size 64, 4 heads for Reddit), and GraphSAGE (3 layers, hidden size
 492 256). All models use layer normalization, ReLU activation functions, and dropout. We performed a
 493 grid search on ogbn-arxiv, ogbn-products, and Reddit to obtain the optimal model hyperparameters
 494 based on final validation accuracy. For ogbn-papers100M we use the same hyperparameters as for
 495 GCN on ogbn-arxiv, but with 32 auxiliary nodes per output node.

496 **Training.** We use the Adam optimizer for all experiments, with a starting learning rate of 10^{-3} . We
 497 use an L_2 regularization of 10^{-4} for GCN on ogbn-arxiv and ogbn-products, and no L_2 regularization
 498 in all other settings. We use a ReduceLROnPlateau scheduler for the optimizer, with the decay factor
 499 0.33, patience 30, minimum learning rate 10^{-4} , and cooldown of 10, based on validation loss. We
 500 train for 300 to 800 epochs and stop early with a patience of 100 epochs, based on validation loss.
 501 We determine the optimal batch order for IBMB via simulated annealing [11].

502 **Training for inference.** For comparing inference performance in Fig. 2 we trained 10 separate
 503 models per setting with node-wise IBMB. We then used the same 10 models to evaluate every method.
 504 Fig. 9 shows that the choice of training method does not impact our findings. The reasons for this are
 505 that the training method (1) does not influence inference time and (2) is not able to bridge the large
 506 accuracy disadvantages that some methods have.

507 **Batch-wise IBMB.** We tune the number of batches and thus the size of batches using a grid search
 508 (see Table 1). Generally, final accuracy increases with larger batch sizes, but this can lead to excessive
 509 memory usage and slower convergence speed. The resulting partitions then define the output nodes in
 510 each batch. We use as many auxiliary nodes as the size of each partition. However, the auxiliary nodes
 511 will be different than the partition since they are selected based on the output nodes via batch-wise
 512 clustering. Note that the inference batch size is double the sizes of training batches since in this case
 513 we do not need to store any gradients.

514 **Node-wise IBMB.** For node-wise batching we first calculate the PPR scores for each output node, and
 515 then pick the top-k nodes as its auxiliary nodes. Generally we use the same batch size, i.e. number
 516 of nodes in a batch, as in batch-wise IBMB, to keep the GPU memory usage similar. However, if
 517 the graph is too dense, we might have to increase the batch size of node-wise IBMB, because it
 518 tends to create sparser batches. We tune the number of auxiliary nodes per output node using a
 519 logarithmic grid search using factors of 2. Based on this we use 16 neighbors for ogbn-arxiv, 64 for
 520 ogbn-products, 8 for Reddit, and 96 for ogbn-papers100M. Note that the number of auxiliary nodes is
 521 the main degree of freedom in IBMB. It influences preprocessing time, runtime, memory usage, and
 522 accuracy. The number of output nodes per batch is then determined by the available GPU memory.

Table 1: Number of batches for batch-wise IBMB.

Model	Dataset	Number of batches		
		Train	Validation	Test
GCN	ogbn-arxiv	4	2	2
GCN	ogbn-products	16	8	8
GCN	Reddit	8	4	4
GAT	ogbn-arxiv	8	4	4
GAT	ogbn-products	1024	512	512
GAT	Reddit	400	200	200
GCN	ogbn-papers100M	256	32	48

Table 2: Hyperparameters for LADIES

Model	Dataset	Nodes per layer	
		Train	Validation
GCN	ogbn-arxiv	42 336	84 672
GCN	ogbn-products	204 085	306 128
GCN	Reddit	90 000	150 000

523 **Approximate PPR.** Calculating the full personalized PageRank (PPR) matrix is prohibitively expen-
 524 sive for large graphs. To enable fast preprocessing times, we approximate node-wise PPR using a
 525 push-flow algorithm [2] with a fixed number of iterations and approximate batch-wise PPR using
 526 power iterations. Both variants are based on parallel sparse matrix operations on GPU. We choose
 527 their hyperparameters so they do not impede accuracy while still having a reasonable preprocessing
 528 time. We use 50 power iterations for batch-wise PPR. For node-wise PPR we use three iterations,
 529 $\epsilon = 0.0002$ for ogbn-arxiv, $\epsilon = 0.0005$ for ogbn-products, and $\epsilon = 0.00002$ for Reddit and ogbn-
 530 papers100M. For node-wise PPR we additionally downsample the unusually dense Reddit adjacency
 531 matrix to an average of 8 neighbors per node.

532 **Random batching.** Random batching is similar to node-wise IBMB except that the auxiliary nodes
 533 are batched randomly. We first calculate the PPR scores and pick the top-k neighbors as the auxiliary
 534 nodes for a output node. We choose the same number of neighbors as with node-wise IBMB. We
 535 investigate 2 variants of random batching: Resampling the batches in every epoch, and sampling
 536 them once during preprocessing and then fixing the batches. We only show the results for the second
 537 method, since we found it to be significantly faster, albeit requiring significantly more main memory.

538 **Hyperparameter tuning.** The priorities for tuning the hyperparameters are as follows: 1. To keep
 539 methods comparable in a realistic setup, we keep the GPU memory usage constant between methods.
 540 2. When there are semantic hyperparameters that do not influence performance (such as the number of
 541 steps per epoch in GraphSAINT-RW, which only changes how an epoch is defined), we choose them
 542 to be comparable to other methods. 3. We choose all relevant hyperparameters based on validation
 543 accuracy. If a hyperparameter is not critical to memory usage we tune it per dataset and not per model.
 544 We use this process for both IBMB and the baselines.

545 **Baseline hyperparameters.** For Cluster-GCN the number of batches are the same as for batch-wise
 546 IBMB. Table 2 shows the hyperparameters for LADIES, Table 3 for neighbor sampling, and Table 4

Table 3: Hyperparameters for neighbor sampling

Model	Dataset	Number of batches			Number of nodes
		Train	Validation	Test	
GCN	ogbn-arxiv	12	8	8	6, 5, 5
GCN	ogbn-products	20	4	200	5, 5, 5
GCN	Reddit	8	4	4	12, 12
GAT	ogbn-arxiv	8	4	4	8, 7, 5
GAT	ogbn-products	1000	150	8000	15, 10, 10
GAT	Reddit	400	400	400	20, 20

Table 4: Hyperparameters for GraphSAINT-RW

Model	Dataset	Walk length	Sample coverage	Number of steps	Batch size	
					Train	Val/Test
GCN	ogbn-arxiv	2	100	4	25 000	10 000
GCN	ogbn-products	2	100	16	80 000	5000
GCN	Reddit	2	100	8	23 000	6000
GAT	ogbn-arxiv	2	100	8	17 500	10 000
GAT	ogbn-products	2	100	1024	14 000	100
GAT	Reddit	2	100	400	1600	60

Table 5: Methods and hyperparameters for selecting auxiliary nodes for GCN on ogbn-products with batch-wise IBMB. IBMB is very robust to this choice. We did observe a slightly lower validation accuracy for low alpha (0.05). We always use 0.25.

Method	α, t	Time (s)	Test accuracy (%)	
		per epoch	IBMB inference	Full-batch
PPR	0.05	3.5	76.8±0.3	77.1±0.3
PPR	0.15	3.6	76.6±0.4	76.9±0.4
PPR	0.25	3.5	76.8±0.2	77.2±0.3
PPR	0.35	3.5	76.9±0.5	77.2±0.5
Heat kernel	0.1	3.5	76.5±0.4	76.8±0.3
Heat kernel	1	3.5	76.6±0.5	76.9±0.5
Heat kernel	3	3.5	76.8±0.2	77.1±0.2
Heat kernel	5	3.5	76.7±0.5	77.0±0.5
Heat kernel	7	3.5	76.6±0.4	76.8±0.4

547 for GraphSAINT-RW. To ensure that every node is visited exactly once during GraphSAINT-RW
 548 inference we use the validation/test nodes only as root nodes of the random walks.

549 **Full-batch inference.** We chunk the adjacency matrix and feature matrix for full-batch inference to
 550 allow using the GPU even for larger datasets. The only hyperparameter is the number of chunks. We
 551 limit the chunk size to ensure that full-batch inference does not exceed the amount of GPU memory
 552 used during training.

553 **Experimental limitations.** We only tested our method on homophilic node classification datasets.
 554 While proximity is a central inductive bias in all GNNs, we did not explicitly test this on a more
 555 general variety of graphs. However, note that IBMB does *not* require homophily. The underlying
 556 assumption is merely that nearby nodes are the most important, not that they are similar. Finally, we
 557 expect our method to perform even better in the context of billion-node graphs, but our benchmark
 558 datasets still fit into main memory.

559 C Ethical considerations

560 Scalable graph-based methods can enable the fast analysis of huge datasets with billions of nodes.
 561 While this has many positive use cases, it also has obvious negative repercussions. It can enable
 562 mass surveillance and the real-time analysis of whole populations and their social networks. This can
 563 potentially be used to detect emerging resistance networks in totalitarian regimes, thus suppressing
 564 chances for positive change. Voting behavior is another typical application of network analysis:
 565 Voters of the same party are likely to be connected to one another. Scalable GNNs can thus influence
 566 voting outcomes if they are leveraged for targeted advertising.

567 The ability of analyzing whole populations can also have negative personal effects in fully democratic
 568 countries. If companies determine credit ratings or college admission based on connected personal
 569 data, a person will be even more determined by their environment than they already are. Companies
 570 might even leverage the obscurity of complex GNNs to escape accountability: It might be easy to
 571 reveal the societal effects of your housing district, but unraveling the combined effects of your social
 572 networks and digitally connected behavior seems almost impossible. Scalable GNNs might thus
 573 make it even more difficult for individuals to escape the attractive forces of the status quo.

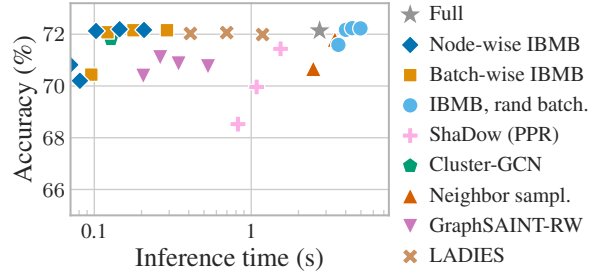


Figure 9: Test accuracy and log. inference time on ogbn-arxiv for 10 GCNs trained with GraphSAINT-RW. The pretraining method does have an impact on the accuracy of some methods, but not enough to change any experimental findings.

Table 6: Main memory usage (GiB). In some settings, IBMB uses more main memory than previous methods due to overlapping batches (e.g. on ogbn-products). However, it can also reduce memory requirements because it ignores irrelevant parts of the graph (e.g. on Reddit). Note that our hyperparameters keep GPU memory usage consistent between methods, as opposed to main memory usage.

	ogbn-arxiv			ogbn-products			Reddit		
	GCN	GAT	GraphSAGE	GCN	GAT	GraphSAGE	GCN	GAT	GraphSAGE
Neighbor sampling	3.0	3.6	3.1	8.7	7.9	8.5	7.4	7.5	7.1
LADIES	3.0	-	-	6.0	-	-	4.8	-	-
GraphSAINT-RW	3.5	3.6	3.5	9.6	9.6	9.6	8.4	8.5	8.4
Cluster-GCN	3.5	3.4	3.5	7.8	6.0	7.3	6.1	4.2	6.5
Batch-wise IBMB	3.5	3.6	3.5	7.9	7.0	7.8	6.3	4.9	6.3
Node-wise IBMB	3.8	3.8	4.2	13.0	12.3	13.2	4.5	5.3	5.1

574 D Additional results

575 **Main memory usage.** IBMB’s main memory usage depends on three aspects: 1. How large is the
 576 training/validation set compared to the full graph? 2. How many auxiliary nodes per output node
 577 are we using? 3. How well are the auxiliary nodes overlapping per batch? As shown in Table 6,
 578 IBMB increases main memory usage in some settings, which is due to the overlap between batches.
 579 However, in other settings it reduces memory requirements because it ignores irrelevant parts of the
 580 graph and removes the dataset from memory after preprocessing. Note that our hyperparameters keep
 581 GPU memory usage consistent between methods.

Table 7: Final accuracy and runtime averaged over 10 runs, with standard deviation. “Same method” refers to using the training method for inference, while “full-batch” uses the whole graph for inference. IBMB achieves similar accuracy as previous methods when used for training, while using significantly less time per epoch and without requiring full-batch inference. IBMB is up to 900x faster (ogbn-papers100M) than using full-batch inference, at comparable accuracy. Other inference methods are substantially slower or less accurate. Note that LADIES is incompatible with the self loops in GAT and GraphSAGE.

Setting	Training method	Time (s)			Test accuracy (%)	
		Preprocess	Per epoch	Inference	Same method	Full-batch
ogbn-arxiv, GCN	Full-batch	-	-	2.8	-	-
	Neighbor sampling	0.3	4.7	2.5	70.7±0.2	71.3±0.4
	LADIES	0.3	0.62	0.69	71.7±0.2	71.4±0.3
	GraphSAINT-RW	0.4	0.42	0.34	68.1±0.2	72.3±0.2
	ShadDow (PPR)	8.3	2.69	1.40	70.9±0.2	72.0±0.1
	Cluster-GCN	8.7	0.14	0.14	72.0±0.1	72.2±0.1
	Batch-wise IBMB	14.1	0.14	0.13	72.2±0.2	72.2±0.2
	Node-wise IBMB	17.5	0.27	0.16	72.6±0.1	72.6±0.1
ogbn-arxiv, GAT	Full-batch	-	-	9.4	-	-
	Neighbor sampling	0.3	4.1	1.97	70.9±0.1	72.1±0.1
	GraphSAINT-RW	0.4	1.2	0.38	68.7±0.2	72.6±0.1
	ShadDow (PPR)	8.4	2.98	1.30	70.3±0.2	71.8±0.1
	Cluster-GCN	7.6	0.69	0.28	69.7±0.3	71.6±0.2
	Batch-wise IBMB	7.7	0.68	0.31	71.0±0.3	71.8±0.3
	Node-wise IBMB	17.6	1.52	0.93	72.0±0.2	72.2±0.2
	ogbn-arxiv, GraphSAGE	Full-batch	-	-	2.37	-
Neighbor sampling		0.3	3.44	1.67	71.1±0.1	72.0±0.1
GraphSAINT-RW		0.3	0.41	0.35	69.0±0.1	72.2±0.1
ShadDow (PPR)		7.7	2.68	1.38	70.9±0.2	71.9±0.2
Cluster-GCN		8.8	0.15	0.14	71.7±0.1	72.1±0.1
Batch-wise IBMB		7.2	0.15	0.13	72.0±0.2	72.1±0.1
Node-wise IBMB		17.5	0.31	0.16	72.4±0.2	72.4±0.1
ogbn-products, GCN		Full-batch	-	-	130	-
	Neighbor sampling	32	42	433	78.2±0.2	78.0±0.2
	LADIES	33	25	22.5	75.9±0.3	79.0±0.4
	GraphSAINT-RW	35	11	20.4	53.6±0.6	79.9±0.2
	ShadDow (PPR)	299	28.5	1242	77.5±0.3	77.4±0.4
	Cluster-GCN	302	3.7	3.4	76.2±0.3	76.5±0.2
	Batch-wise IBMB	306	3.5	3.1	76.8±0.2	77.2±0.3
	Node-wise IBMB	382	5.4	13.8	77.3±0.3	77.3±0.3
ogbn-products, GAT	Full-batch	-	-	1700	-	-
	Neighbor sampling	33	450	3450	79.1±0.3	77.2±0.5
	GraphSAINT-RW	35	140	102	69.5±0.1	80.8±0.2
	ShadDow (PPR)	298	66	1461	77.3±0.3	79.2±0.4
	Cluster-GCN	626	24	10.6	76.6±0.4	78.1±0.5
	Batch-wise IBMB	767	25	10.0	77.0±0.4	78.9±0.6
	Node-wise IBMB	378	42	97	78.9±0.3	79.0±0.3
	ogbn-products, GraphSAGE	Full-batch	-	-	88.0	-
Neighbor sampling		31.4	52.0	530	81.0±0.2	81.4±0.2
GraphSAINT-RW		35.8	10.6	20.0	69.4±0.2	81.3±0.2
ShadDow (PPR)		298	28.3	1169	80.0±0.3	80.8±0.3
Cluster-GCN		313	3.1	3.4	79.5±0.4	79.7±0.4
Batch-wise IBMB		319	2.9	3.1	79.2±0.3	79.5±0.3
Node-wise IBMB		374	5.1	13.3	80.6±0.3	80.8±0.3

Continued on the next page.

Final accuracy and runtime averaged over 10 runs, continued.

Setting	Training method	Time (s)			Test accuracy (%)	
		Preprocess	Per epoch	Inference	Same method	Full-batch
Reddit, GCN	Full-batch	-	-	14.8	-	-
	Neighbor sampling	14.4	7.3	3.3	93.5±0.1	94.8±0.1
	LADIES	15.4	11.4	11.4	95.5±0.0	95.3±0.0
	GraphSAINT-RW	17.1	14.6	2.9	93.2±0.1	95.6±0.0
	ShaDow (PPR)	54.0	7.4	2.2	95.2±0.1	95.0±0.0
	Cluster-GCN	175	1.8	1.6	93.7±0.2	94.8±0.1
	Batch-wise IBMB	175	1.6	1.4	93.5±0.4	94.7±0.1
	Node-wise IBMB	64.8	0.74	0.59	95.7±0.1	95.2±0.1
Reddit, GAT	Full-batch	-	-	76.9	-	-
	Neighbor sampling	14.8	70	32.5	94.3±0.1	95.1±0.1
	GraphSAINT-RW	17.9	21	3.2	79.4±0.2	95.4±0.1
	ShaDow (PPR)	56.5	7.0	1.7	94.6±0.1	94.1±0.2
	Cluster-GCN	366	4.7	1.4	91.4±0.1	93.5±0.7
	Batch-wise IBMB	396	4.3	1.2	91.6±0.1	92.8±1.1
	Node-wise IBMB	65.3	1.1	0.25	94.2±0.1	94.1±0.3
Reddit, GraphSAGE	Full-batch	-	-	17.3	-	-
	Neighbor sampling	16.1	7.5	3.5	96.2±0.0	96.8±0.0
	GraphSAINT-RW	18.2	14.6	3.6	95.9±0.0	96.8±0.0
	ShaDow (PPR)	56.5	7.3	2.4	96.8±0.0	96.4±0.0
	Cluster-GCN	173	1.7	1.8	95.5±0.2	96.0±0.1
	Batch-wise IBMB	175	1.6	1.7	95.6±0.2	96.1±0.1
Node-wise IBMB	66.0	0.78	0.65	96.8±0.0	96.5±0.0	
papers 100M, GCN	Full-batch	-	-	5700	-	-
	Neighbor sampling	739	900	159	64.3±0.2	61.8±0.2
	LADIES	735	2830	672	65.4±0.2	62.4±0.4
	Node-wise IBMB	2290	51	6.2	66.1±0.1	66.0±0.1